



Identification of a Putative Sensor Protein Involved in Regulation of Vesicle Production by a Hypervesiculating Bacterium, *Shewanella vesiculosa* HM13

Fumiaki Yokoyama^{1†}, Tomoya Imai², Wataru Aoki^{3,4}, Mitsuyoshi Ueda^{3,4}, Jun Kawamoto¹ and Tatsuo Kurihara^{1*}

¹ Institute for Chemical Research, Kyoto University, Uji, Japan, ² Research Institute for Sustainable Humanosphere, Kyoto University, Uji, Japan, ³ Division of Applied Life Sciences, Graduate School of Agriculture, Kyoto University, Kyoto, Japan, ⁴ Kyoto Integrated Science and Technology Bio-Analysis Center, Kyoto, Japan

OPEN ACCESS

Edited by:

Masahiro Ito,
Toyo University, Japan

Reviewed by:

Masanori Toyofuku,
University of Tsukuba, Japan
Yosuke Tashiro,
Shizuoka University, Japan

*Correspondence:

Tatsuo Kurihara
kurihara@scl.kyoto-u.ac.jp

† Present address:

Fumiaki Yokoyama,
Bioanalytics Group, Department
of Biosystems Science
and Engineering, ETH Zurich, Basel,
Switzerland

Specialty section:

This article was submitted to
Extreme Microbiology,
a section of the journal
Frontiers in Microbiology

Received: 13 November 2020

Accepted: 29 January 2021

Published: 18 February 2021

Citation:

Yokoyama F, Imai T, Aoki W,
Ueda M, Kawamoto J and Kurihara T
(2021) Identification of a Putative
Sensor Protein Involved in Regulation
of Vesicle Production by
a Hypervesiculating Bacterium,
Shewanella vesiculosa HM13.
Front. Microbiol. 12:629023.
doi: 10.3389/fmicb.2021.629023

Bacteria secrete and utilize nanoparticles, called extracellular membrane vesicles (EMVs), for survival in their growing environments. Therefore, the amount and components of EMVs should be tuned in response to the environment. However, how bacteria regulate vesiculation in response to the extracellular environment remains largely unknown. In this study, we identified a putative sensor protein, HM1275, involved in the induction of vesicle production at high lysine concentration in a hypervesiculating Gram-negative bacterium, *Shewanella vesiculosa* HM13. This protein was predicted to possess typical sensing and signaling domains of sensor proteins, such as methyl-accepting chemotaxis proteins. Comparison of vesicle production between the *hm1275*-disrupted mutant and the parent strain revealed that HM1275 is involved in lysine-induced hypervesiculation. Moreover, HM1275 has sequence similarity to a biofilm dispersion protein, BdlA, of *Pseudomonas aeruginosa* PAO1, and *hm1275* disruption increased the amount of biofilm. Thus, this study showed that the induction of vesicle production and suppression of biofilm formation in response to lysine concentration are under the control of the same putative sensor protein.

Keywords: extracellular membrane vesicles, biofilm, *Shewanella*, cold-adapted bacterium, sensor protein

INTRODUCTION

Bacterial cells respond to extracellular environments, create multicellular communities, and communicate with others for survival in their growing environments. To communicate, they secrete and utilize nanoparticles, called extracellular membrane vesicles (EMVs) (Schwechheimer and Kuehn, 2015). Therefore, the amount and components of EMVs should be tuned in response to the environment (Orench-Rivera and Kuehn, 2016). EMVs are composed of various components, such as lipids, proteins, nucleic acids, lipopolysaccharides, and peptidoglycans (Bitto and Kaparakis-Liaskos, 2017). Major components of EMVs of Gram-negative bacteria are derived from the outer membrane and periplasm of the cells, while components of the inner membrane and cytoplasm are also found in EMVs from various bacterial species

(Toyofuku et al., 2015; Jain and Pillai, 2017; Tan et al., 2018). Owing to the diversity of these components, EMVs have various physiological roles, being involved in biofilm formation, nutrient uptake, defense (acting as decoys against bacteriophages), and intercellular communication related to horizontal gene transfer and pathogenesis (Toyofuku et al., 2015). Moreover, EMVs have been applied to the development of vaccines and drug delivery systems (Jain and Pillai, 2017; Tan et al., 2018). Elucidation of the vesiculation mechanisms is required for the understanding of their physiology and the development of their applications. Although multiple mechanisms of vesicle production have been suggested to occur in various bacteria (Schwechheimer and Kuehn, 2015; Toyofuku et al., 2015), it remains largely unclear how bacteria regulate the production levels of EMVs in response to extracellular environments.

We previously isolated a bacterial strain suitable for studies of EMVs. This strain, *Shewanella vesiculosa* HM13, is a Gram-negative and cold-adapted bacterium that was isolated from horse mackerel intestines (Chen et al., 2020). Vesiculation by this bacterium has two unique features: higher vesicle production than other strains such as *Escherichia coli* and high purity and productivity of a single specific protein in EMVs; these characteristics make *S. vesiculosa* HM13 useful for elucidating the mechanisms of bacterial vesiculation and protein transport to EMVs (Chen et al., 2020; Guida et al., 2020; Kamasaka et al., 2020; Kawano et al., 2020).

In this study, we identified a putative sensor protein in *S. vesiculosa* HM13 EMVs that harbors sensory Per-Arnt-Sim (PAS) domains and a signaling domain of a methyl-accepting chemotaxis protein (MCP). This protein showed sequence similarity to a biofilm dispersion protein, BdlA, of *Pseudomonas aeruginosa* PAO1 (Morgan et al., 2006; Barraud et al., 2009; Petrova and Sauer, 2012). Gene disruption and quantification of EMVs and biofilm showed that this protein is involved in the sensing of lysine (Lys) in the extracellular environment to induce vesicle production and regulate biofilm formation.

MATERIALS AND METHODS

Bacterial Strains and Culture Conditions

The strains used in this study are listed in Table 1. A cold-adapted bacterium, *S. vesiculosa* HM13, was isolated from the intestines of horse mackerel, and a rifampicin-resistant mutant of this strain (HM13-Rif^r) was used as a parental strain (Chen et al., 2020). A mutant (Δ *gspD2*) lacking a protein required for the transport of a major EMV cargo protein, P49, was used to identify minor proteins included in EMVs (Chen et al., 2020). Another mutant lacking a putative sensor protein encoded by *hm1275* was prepared by gene disruption using a pKNOCK plasmid (Table 1). In brief, a linear fragment of pKNOCK, amplified with the primers pKNOCK-1 and -2 (Table 2), was fused with the internal fragment of *hm1275*, amplified with the primers Dh1275-1 and -2 (Table 2) using a NEBuilder HiFi DNA Assembly Kit (New England Biolabs, Ipswich, MA, United States) according to the manufacturer's instructions. *S. vesiculosa* HM13-Rif^r was conjugated with *E. coli*

TABLE 1 | Bacterial strains and plasmids used in this study.

Strain or plasmid	Description	References
Strains		
<i>E. coli</i>		
S17-1/ λ <i>pir</i>	<i>E. coli</i> S17-1 derivative, host for <i>pir</i> -dependent plasmids	Simon et al., 1983
<i>S. vesiculosa</i>		
HM13-Rif ^r	Parental strain, rifampicin resistant mutant of <i>S. vesiculosa</i> HM13	Chen et al., 2020
Δ <i>gspD2</i>	<i>hm3349</i> -disrupted mutant (<i>hm3349</i> :pKNOCK) of HM13-Rif ^r	Chen et al., 2020
Δ <i>hm1275</i>	<i>hm1275</i> -disrupted mutant (<i>hm1275</i> :pKNOCK) of HM13-Rif ^r	This work
Plasmids		
pKNOCK	Km ^r	Alexeyev, 1999
pJRD-Cm ^r	Cm ^r ; A pJRD215 derivative with Cm ^r instead of Km ^r	Toyotake et al., 2018
<i>phm1275</i>	Cm ^r ; A pJRD-Cm ^r derivative containing <i>hm1275</i> at the <i>MluI</i> - <i>SpeI</i> site	This work

TABLE 2 | Primers used in this study.

Primers	Sequence	Target gene
pKNOCK-1	GATATCAAGCTTATCGATACCG	pKNOCK
pKNOCK-2	CACTAGTTCTAGAGCGGC	As above
pJRD-Cm ^r -1	TAGTATAGTCTATAGTCCGTGG	pJRD-Cm ^r
pJRD-Cm ^r -2	CGTAATCCATGGATCAAGAG	As above
Dh1275-1	<u>CGGCCGCTCTAGA</u> <u>ACTAGT</u> <u>G</u> GCGCCAGAGGAACAGCTC	<i>hm1275</i>
Dh1275-2	<u>GTATCGATAAGCTT</u> <u>GATA</u> CAATCCTGTAGTGTCTTGT	As above
Ch1275-1	<u>CTCTTGATCCATGGATT</u> <u>ACG</u> GTTTTAATGAGTAATCTAACTCCAC	As above
Ch1275-2	<u>CCACGGACTATAGACTATACTA</u> TTAAGTATTGAGTTGATTGGCAA	As above

The sequences overlapping those of the vectors are underlined.

S17-1/ λ *pir* transformed with the plasmid and then selected on a 1.5% lysogeny broth (LB) agar plate with rifampicin (Rif, 50 μ g/mL) and kanamycin (Km, 50 μ g/mL) to obtain the mutant Δ *hm1275*. The HM13-Rif^r strain and all mutants were subcultured from seed culture using fresh media (1:100 dilution rate) without antibiotics. For the complementation assay of *hm1275*, an empty vector-introduced strain, Δ *hm1275*/p, and the complemented strain, Δ *hm1275*/*phm1275*, were prepared as described below in the section "Construction of Complemented Strain." After cultivation, the mutants and empty vector-introduced/complemented strains were plated onto a 1.5% LB agar plate with Rif (50 μ g/mL) and Km (50 μ g/mL), or with Rif, Km, and chloramphenicol (Cm, 30 μ g/mL), respectively, to confirm the maintenance of the plasmid and the plasmid-derived sequence in the genome.

To investigate the effects of the growth environment on vesiculation, three media were used: LB, modified DSMZ medium 79 (M79 medium) (Papa et al., 2006), and Bacto Marine Broth (MB) (Difco Laboratories, Detroit, MI, United States). The M79

medium contained 1 g/L KH_2PO_4 , 1 g/L NH_4NO_3 , 10 g/L NaCl, 0.2 g/L $\text{MgSO}_4 \cdot 7\text{H}_2\text{O}$, 10 mg/L FeSO_4 , 10 mg/L $\text{CaCl}_2 \cdot 2\text{H}_2\text{O}$, and 0.5% w/v casamino acid (CA). M79 medium supplemented with additional CA or Lys (hereafter, M79 + CA or M79 + Lys, respectively) was also used to investigate the effects of amino acids on vesiculation. HM13-Rif^r and $\Delta hm1275$ were grown at 18°C and 180 rpm in a Bio Shaker BR-43FL (TAITEC CORPORATION, Saitama, Japan) until the cultures reached the early stationary phase. The optical density at 600 nm (OD_{600}) was measured with a UV-visible spectrophotometer (UV-2450, Shimadzu, Kyoto, Japan). The growth curve was obtained using a rocking incubator TVS062CA (ADVANTEC, Tokyo, Japan) at 18°C and 70 rpm.

Construction of Complemented Strain

A DNA fragment including the estimated promoter region and coding region of *hm1275* was obtained by PCR with Q5 High-Fidelity DNA Polymerase (New England Biolabs) using *S. vesiculosa* HM13 genomic DNA as a template and the primers Chm1275-1 and -2 (Table 2). The resulting DNA fragment and linearized pJRD-Cm^r (Toyotake et al., 2018), prepared by PCR with the primers pJRD-Cm^r-1 and -2 (Table 2), were fused to construct pJRD-Cm^r/*hm1275* using a NEBuilder HiFi DNA Assembly Kit, according to the manufacturer's instructions. $\Delta hm1275$ was conjugated with *E. coli* S17-1/ λ -pir, transformed with pJRD-Cm^r/*hm1275* or the empty vector pJRD-Cm^r, and then selected on a 1.5% LB agar plate with Rif (50 $\mu\text{g}/\text{mL}$), Km (50 $\mu\text{g}/\text{mL}$), and Cm (30 $\mu\text{g}/\text{mL}$) to obtain a complemented strain and the empty vector-introduced strain, $\Delta hm1275/p hm1275$ and $\Delta hm1275/p$, respectively.

Isolation of EMVs by Ultracentrifugation

EMVs from *S. vesiculosa* HM13 were collected from cultures at the early stationary phase, unless otherwise stated, according to a previously described method (Yokoyama et al., 2017) with slight modifications. In brief, the cells were pelleted by centrifugation at $6,800 \times g$ and 4°C for 10 min. The supernatant was centrifuged at $13,000 \times g$ and 4°C for 15 min to remove the remaining bacterial cells. The supernatant was filtered through a 0.45- μm pore polyethersulfone (PES) filter to remove the remaining debris. EMVs were obtained by ultracentrifugation from 4 mL of filtrate at $100,000 \times g$ (average centrifugal force) and 4°C for 2 h with an Optimax centrifuge (Beckman Coulter, Brea, CA, United States). The pellets were resuspended in 400 μL of Dulbecco's phosphate-buffered saline (DPBS) (Manning and Kuehn, 2011) and used as EMVs in the following experiments. The post-ultracentrifuged supernatant without EMVs was kept as a post-vesicle fraction (PVF) for subsequent experiments.

Vesicle Quantification by Lipid Staining

Lipids in the EMV fractions were quantified with a lipophilic fluorescent molecule, FM4-64 (Molecular Probes/Thermo Fisher Scientific, Waltham, MA, United States). The fluorescence intensities were divided by the OD_{600} values of the cultures for normalization to quantify vesicle production, according to previously described methods (Yokoyama et al., 2017). To examine the effects of Lys concentration on vesicle production,

EMVs of HM13-Rif^r, statically cultured at 18°C for 3 days in 5 mL of M79 media with different Lys concentrations, were quantified as described above. The maximum concentration of Lys in this study (2.6 g/L) is supposed to be physiologically relevant and comparable to the one found in the intestine of horse mackerel, the host of *S. vesiculosa* HM13, which consumes krill as its main diet (Huntley et al., 1994; Chen et al., 2009; Kolmakova and Kolmakov, 2019).

Protein Identification by Peptide Mass Fingerprinting

Proteins associated with EMVs (600 μg) of $\Delta gspD2$ aerobically cultured in LB were identified by two-dimensional polyacrylamide gel electrophoresis (2D-PAGE) and peptide mass fingerprinting, according to previously described methods (Park et al., 2012) with slight modifications. The peptide mass spectra of each protein spot were subjected to MASCOT search (Matrix Science, London, United Kingdom) against the *S. vesiculosa* HM13 protein database. The identified proteins were profiled using BLAST¹ (Altschul et al., 1997) and HHpred² (Söding et al., 2005). The localizations of the identified proteins were predicted using PSORTb version 3.0.2³ (Yu et al., 2010) and are listed in Table 3.

Quantification of Biofilm by Crystal Violet Staining

The cells attached to the solid surface were stained with crystal violet (CV) to quantify the amount of biofilm, according to previously described methods (Thormann et al., 2004) with slight modifications. In brief, the cells were grown statically in 150 μL of M79 medium with CA or amino acid supplementation in a 96-well U-bottom plate (Delta Lab, Barcelona, Spain) at the optimal growth temperature for HM13-Rif^r (18°C) for 3 days. After cultivation, the floating cells were removed, and the remaining cells attached to the plate were washed twice with 170 μL of water. After drying the plate at room temperature for approximately 5 min, 170 μL of 0.1% CV aq. was added to the wells and incubated at room temperature for 30 min. After the staining solution was removed, the wells were washed twice with 300 μL of water. Then, the cells were destained with 170 μL of 95% ethanol (Nacalai Tesque, Kyoto, Japan) by incubation at room temperature for 30 min. One hundred microliters of the destaining solution were applied to a 96-well flat-bottom plate (Delta Lab) to measure the absorbance at 570 nm with a plate reader (SpectraMax 190, Molecular Devices, San Jose, CA, United States).

Biofilm Observation by Scanning Electron Microscopy

To observe the fine structure of the biofilm formed at the air-liquid interface, the biofilm formed on a glass strip was subjected to scanning electron microscopy (SEM), according

¹<http://www.ncbi.nlm.nih.gov/blast>

²<https://toolkit.tuebingen.mpg.de/tools/hhpred>

³<http://www.psort.org/psortb/>

TABLE 3 | The identified proteins in EMVs from *ΔgspD2*.

No. ^a	Gene	Function of the protein predicted by its sequence	Calculated mass (mass/Da)	Calculated pI	E-value ^b	Localization ^c	Accession
1	<i>hm67</i>	Siderophore biosynthesis protein PvsD	73,079	6.38	4.8×10^{-2}	IM	LC533412
2	<i>hm433</i>	50S ribosomal protein L	20,230	9.38	4.2×10^{-2}	C	LC533413
3	<i>hm594</i>	HDOD domain-containing protein	30,072	5.14	3.6×10^{-2}	C	LC533414
4	<i>hm679</i>	DNA-directed RNA polymerase omega subunit	10,081	4.97	7.6×10^{-3}	C	LC533415
5	<i>hm841</i>	Mechanosensitive ion channel family protein	21,250	10.2	1.3×10^{-2}	IM	LC533416
6	<i>hm858</i>	Lysine-sensitive aspartokinase 3	50,020	5.51	4.0×10^{-2}	C	LC533417
7	<i>hm1275</i>	Methyl-accepting chemotaxis protein	49,116	5.99	3.3×10^{-2}	IM	LC533418
8	<i>hm1305</i>	Zinc chelation protein SecC	39,225	8.58	3.1×10^{-2}	Not predictable	LC533419
9	<i>hm1390</i>	Error-prone, lesion bypass DNA polymerase V (UmuC)	47,001	9.36	5.1×10^{-2}	C	LC533420
10	<i>hm1529</i>	Hypothetical protein	23,709	9.03	3.2×10^{-4}	Not predictable	LC533421
11	<i>hm2195</i>	tRNA (carboxy-S-adenosyl-L-methionine) synthase CmoA	26,476	5.49	3.6×10^{-2}	C	LC533422
12	<i>hm2235</i>	Glucose-1-phosphate adenylyltransferase	46,828	6.28	4.5×10^{-2}	Not predictable	LC533423
13	<i>hm3132</i>	Pyruvate oxidase	45,665	5.69	4.8×10^{-2}	IM	LC533424
14	<i>hm3337</i>	Hypothetical protein	18,135	9.92	4.5×10^{-2}	IM	LC533425
15	<i>hm3779</i>	RNA polymerase-binding protein DksA (C4-type zinc finger protein)	16,848	5.21	5.4×10^{-2}	C	LC533426

^a Annotated spot numbers indicated in **Figure 2**.

^b The E-value is the number of hits expected with a similar score by chance when searching the database with the amino acid sequence of each protein.

^c The subcellular localization of each protein was predicted using a subcellular localization prediction tool, PSORTb version 3.0.2. IM, inner membrane; C, cytoplasm.

to previously described methods (Iwamoto et al., 2007) with slight modifications. In brief, cells in 500 μ L of M79 medium with 0.5% CA containing a glass strip along the wall of a 24-well plate (AGC, Tokyo, Japan) were fixed with 2% glutaraldehyde (Wako Pure Chemical Industries, Osaka, Japan), stained with OsO₄ (Nisshin EM Co., Ltd., Tokyo, Japan), subjected to solvent exchange, and lyophilized overnight. The cells on the glass strip were then coated with platinum (approximately 2 nm) using an auto-fine coater (JEC-3000, JEOL, Tokyo, Japan), and observed with a field-emission SEM, JSM-7800F Prime (JEOL), at an acceleration voltage of 5 kV, according to previously described methods (Iwamoto et al., 2007).

Biofilm Observation by Confocal Laser Scanning Microscopy

Biofilms of HM13-Rif^r and the mutant were observed by confocal laser scanning microscopy (CLSM), according to previously described methods (Sabaeifard et al., 2017) with slight modifications. In brief, biofilms on a glass-base dish (AGC), obtained by static cultivation at 18°C for 3 days in 2 mL of M79 medium supplemented with 0.5% CA, were washed with DPBS twice, then stained with 1000-fold diluted propidium iodide and SYTO 9 (LIVE/DEAD[®] BacLight[™] Bacterial Viability Kit, Molecular Probes/Thermo Fisher Scientific) at room temperature in darkness for 15 min. The biofilms were observed at the air-liquid interface by CLSM using a 60 \times objective (FV3000, Olympus, Tokyo, Japan) with an excitation laser at 488 nm.

Quantification and Visualization of Biofilm With BiofilmQ

The biofilm images from three frames obtained by CLSM were quantified, and representative images were modeled with the biofilm analysis software BiofilmQ⁴, and the image software ParaView⁵, according to previously described methods (Hartmann et al., 2019).

Protein Identification by Proteome Analysis

Cells of *S. vesiculosa* HM13, statically cultured in 5 mL of M79 media with 0.26 and 2.6 g/L Lys at 18°C for 3 days, were homogenized by sonication in lysis buffer (7 M urea, 2 M thiourea, 2% 3-[(3-cholamidopropyl)-dimethylammonio]-1-propanesulfonate, 10 mM dithiothreitol, and 50 mM Tris-HCl (pH 7)). The homogenate was centrifuged at 20,000 \times g at 4°C for 20 min to remove any remaining debris. The solvent was exchanged with 100 mM triethylammonium bicarbonate (pH 8.5) with Amicon Ultra-0.5 (10-MWCO, Millipore, Billerica, MA, United States). Tris(2-carboxyethyl)phosphine (0.2 M) was added to the sample, which was then incubated at 55°C for 60 min. For alkylation, 375 mM 2-iodoacetamide was added, and the sample was incubated at room temperature in darkness for 30 min. Then, cold acetone was added to the sample, which was then incubated at -30°C for 3 h. Next, the sample was centrifuged at 4°C and 20,300 \times g for 15 min, dried at room temperature, and then suspended in 50 mM triethylammonium bicarbonate. The proteins in the sample

⁴<https://drescherlab.org/data/biofilmQ/docs/index.html>

⁵<https://www.paraview.org/>

were digested with 10 $\mu\text{g}/\text{mL}$ sequence grade modified trypsin (Promega Corporation, Madison, WI, United States) at 37°C overnight. The digested proteins were labeled by incubation with TMT Mass Tagging Kits and Reagents (Thermo Fischer Scientific, Rockford, IL, United States) in dehydrated acetonitrile at room temperature for 1 h. Then, 5% hydroxylamine was added to the sample, which was then incubated at room temperature for 15 min. Finally, the sample was frozen with liquid nitrogen and stored at -80°C for proteome analysis.

The proteins in the sample were subjected to tandem mass tag-labeling proteomic analysis, according to previously described methods (Tsuji et al., 2020). Proteins were identified by MASCOT search against the *S. vesiculosa* HM13 protein database. The fold-change values were determined as peptide abundance ratios between the cells grown with 0.26 and 2.6 g/L Lys. The global median normalization method was used to normalize the amount of tryptic digests subjected to the analysis. Changes with *p*-values lower than 0.05 were considered statistically significant, and the corresponding genes were annotated by BLAST search and are listed in **Table 4**.

RESULTS

Variation of Vesiculation Depending on Extracellular Environment

To investigate whether *S. vesiculosa* HM13 regulates vesiculation in response to the extracellular environment, EMVs of this strain cultured in different media were characterized. We used the following three culture media: the rich nutrient LB, a minimal synthetic M79 medium (Papa et al., 2006), and MB, which is generally used for cultivating heterotrophic marine bacteria. The amount of EMVs at the early stationary phase ($\text{OD}_{660} \approx 2.5$ in LB and 2.0 in M79 medium and MB) (**Supplementary Figure 1A**) was quantified by lipid staining (**Figure 1**), which showed that this strain cultured in the nutrient-poor conditions of M79 medium produced fewer EMVs than in the rich nutrient LB, and the amount of EMVs in MB was much lower than that in the other media. Consistent with a previous study (Chen et al., 2020), this strain cultured in LB produced a single major protein, P49, in the EMV fraction, while other proteins were barely visible in both the EMV fraction and the PVF, the latter consisting of the supernatant obtained after ultracentrifugation to remove EMVs (**Supplementary Figure 1B**). Conversely, in M79 medium and MB, P49 was detected in both EMV fractions and PVFs (**Supplementary Figure 1B**).

Identification of a Sensor Protein in EMVs

To further characterize EMVs and obtain insights into the mechanism of their biogenesis, proteins in EMVs of the *gspD2*-disrupted mutant (ΔgspD2) were identified by gel-based proteomics. For this experiment, ΔgspD2 , which lacks a putative outer membrane conduit for transport of P49 to EMVs, was used as the disruption of *gspD2* does not impair the production of EMVs (Chen et al., 2020; Kamasaka et al., 2020) and facilitates

the identification of minor cargo proteins of EMVs owing to the absence of the major cargo protein P49. Indeed, in EMVs from the parental strain, the amount of P49 is much higher than that of other proteins, and this phenomenon prevents the identification of other proteins by 2D-PAGE owing to the limited protein-loading capacity of the gel.

EMVs from ΔgspD2 were subjected to 2D-PAGE (**Figure 2**), and protein spots indicated by the black arrowheads in **Figure 2** were identified by peptide mass fingerprinting (**Table 3**). It is noteworthy that most of them were predicted to be cytosolic and inner membrane proteins; in fact, proteins estimated to localize in the cytoplasm and inner membranes are often found in EMVs (Toyofuku et al., 2015; Jain and Pillai, 2017; Tan et al., 2018). This fact may be at least partially explained by the occurrence of outer-inner membrane vesicles (O-IMVs) secreted by various Gram-negative bacteria (Pérez-Cruz et al., 2013, 2015, 2016).

Among these proteins, that encoded by *hm1275* (spot #7 in **Figure 2**) was profiled using BLAST (Altschul et al., 1997) and HHpred (Söding et al., 2005), which showed that this protein has structural features similar to those of a typical bacterial MCP, which carries a PAS domain to sense signals (Henry and Crosson, 2011) and an MCP signaling domain that interacts with other downstream proteins (**Supplementary Table 1**; Falke et al., 1997; Ud-Din and Roujeinikova, 2017). Although proteins that contain PAS and MCP domains generally play a role in signal transduction followed by chemotaxis (Henry and Crosson, 2011), some of these chemosensory components regulate non-chemotaxis-related functions (Wadhams and Armitage, 2004). For example, MCPs have been reported to be involved not only in motility, but also in other bacterial functions, including virulence and biofilm formation (Choi et al., 2015); thus, experimental data are needed to elucidate the function of HM1275. Since HM1275 was predicted to be a membrane protein using PSORTb (Yu et al., 2010), its properties may have caused its abnormal migration in 2D-PAGE, where its apparent molecular mass differed from the calculated mass reported in **Table 3**; in fact, this phenomenon also occurred for other membrane proteins (Rath et al., 2009; Rath and Deber, 2013).

Induction of Vesicle Production Mediated by a Putative Sensor Protein, HM1275, in the Presence of a High Concentration of Lys

We then examined whether HM1275 senses signal molecules in the extracellular environment and regulates vesicle production. To facilitate the identification of a signal molecule that affects vesicle production, a totally synthetic and nutrient-poor M79 medium was used for this experiment. Within its components, we focused on amino acids, previously reported as signal molecules for MCPs in bacteria (Springer et al., 1977; Hedblom and Adler, 1980; Hanlon and Ordal, 1994). In particular, we focused on the concentration of Lys, which is abundant in zooplankton (Kolmakova and Kolmakov, 2019). The latter is the most typical diet of horse mackerel (Jardas et al., 2004), from whose intestines *S. vesiculosa* HM13 was isolated (Chen et al., 2020). Therefore, we hypothesized that Lys concentration may be sensed by this

TABLE 4 | Change of protein expression in response to Lys concentration.

Gene	Fold change ^a	Protein ^b	p-value ^c	Accession
hm3452	1.59	SSU ribosomal protein S16p	1.8×10^{-2}	LC533463
hm2439	1.38	Cytochrome c oxidase subunit CcoO	4.6×10^{-2}	LC547421
hm1357	0.56	Cell division protein BolA	7.7×10^{-3}	LC547422
hm4008	0.54	Hypothetical protein	7.7×10^{-3}	LC547423
hm498	0.52	Isoquinoline 1-oxidoreductase alpha subunit	3.4×10^{-2}	LC547424
hm4042	0.51	TRAP transporter solute receptor, unknown substrate 1	3.8×10^{-2}	LC547425
hm3656	0.50	Hypothetical protein	2.0×10^{-2}	LC547426
hm4030	0.50	Methionine repressor MetJ	4.8×10^{-2}	LC533496
hm244	0.46	Secreted and surface protein containing fasciclin-like repeats	9.5×10^{-3}	LC533506
hm1567	0.45	Hypothetical protein	3.8×10^{-2}	LC533509
hm810	0.22	Hypothetical protein	3.6×10^{-4}	LC533516
hm2742	0.20	Cold shock protein CspD	1.2×10^{-2}	LC533517
hm4032	0.18	Cytochrome c family protein	4.1×10^{-2}	LC533518

^aFold changes were calculated by dividing the average expression values relative to 2.6 g/L Lys-grown cells by those of 0.26 g/L Lys-grown cells.

^bProteins in the database showing the highest sequence similarity to the proteins from *S. vesiculosa* HM13.

^cThe p-value was calculated using two-tailed unpaired Student's t-test to evaluate the difference between the relative abundance of each protein expressed in 0.26 and 2.6 g/L Lys-grown cells.

strain as a marker of environmental change caused by food intake by the host; thus, we cultivated bacterial cells in media containing Lys at physiological concentrations (up to 2.6 g/L) for subsequent experiments (for details, please refer to the “Materials and Methods” section).

An *hm1275*-disrupted strain ($\Delta hm1275$) was prepared as described in the “Materials and Methods” section. The growth of this strain was similar to that of its parental strain (HM13-Rif^r) in M79 + CA (Supplementary Figure 2). Next, these two strains were cultured in modified M79 media supplemented with different concentrations of Lys. The relative vesicle production of HM13-Rif^r, quantified by lipid staining, increased in a Lys concentration-dependent manner (Figure 3). Similar tendencies were observed by nanoparticle tracking analysis (Supplementary Figure 3A; Filipe et al., 2010). Lys concentration-dependent increase in the growth was also observed, but it was less significant than that in the vesicle production (Supplementary Figure 4). EMVs produced under these conditions had similar mean diameters, although smaller EMVs were more abundant in the presence of 1.3 g/L Lys than in other conditions (Supplementary Figure 3B). Notably, HM13-Rif^r cultured in M79 medium with 2.6 g/L Lys produced an approximately four-fold larger number of EMVs compared to the same strain grown in original M79 medium containing 0.26 g/L Lys. However, Lys-induced vesicle production by $\Delta hm1275$ was significantly lower than that of HM13-Rif^r (Figure 3). Nevertheless, under all conditions, transmission electron microscopy did not reveal any morphological differences between EMVs from these strains (Supplementary Figure 5). Effects of the *hm1275* disruption on the Lys-dependent growth increase were also less significant than those on the Lys-induced vesicle production (Supplementary Figure 4).

To confirm that the suppression of the Lys-induced vesicle production (Figure 3) was caused by the disruption of *hm1275*, the complemented strain of $\Delta hm1275$ ($\Delta hm1275/phm1275$) and an empty vector-introduced strain ($\Delta hm1275/p$) were used. In

M79 media with 2.6 g/L Lys, the relative vesicle production of $\Delta hm1275/phm1275$ was significantly higher than that of $\Delta hm1275/p$ (Supplementary Figure 6), suggesting that the disruption of *hm1275* caused the observed phenotype.

Repression of HM1275-Dependent Biofilm Formation

To adapt to the extracellular environment, bacteria accurately control the transition between planktonic and biofilm states (Rossi et al., 2018). Interestingly, pairwise alignment of amino

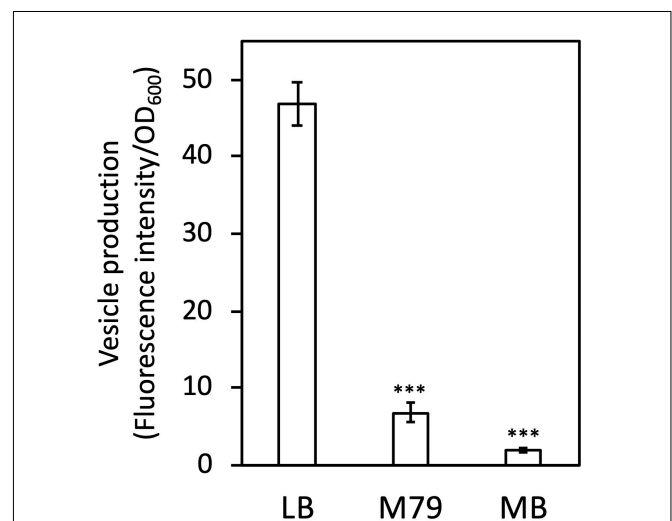
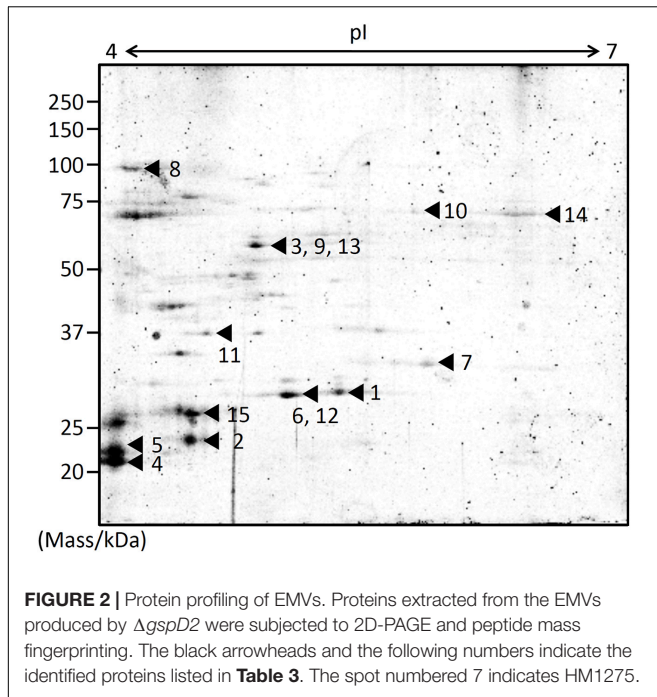


FIGURE 1 | Vesicle productivity of *S. vesiculosa* HM13 in different media. EMVs of *S. vesiculosa* HM13 cultured in different media were quantified by lipid staining with a lipophilic fluorescent molecule, FM4-64. The data are the means \pm standard errors of the values from three independent batches. Statistical analysis was performed using two-tailed unpaired Student's t-test. *** indicates $p < 0.01$, compared with LB.

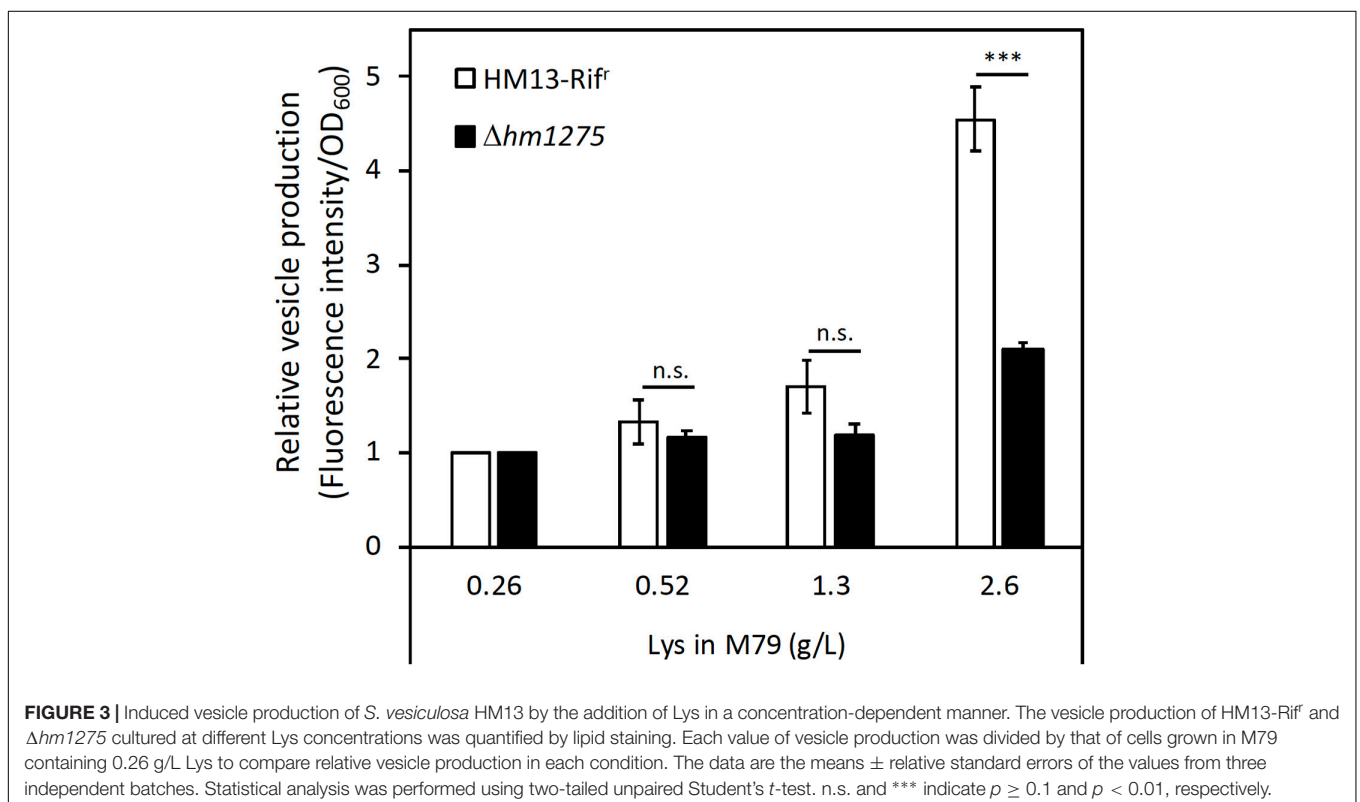


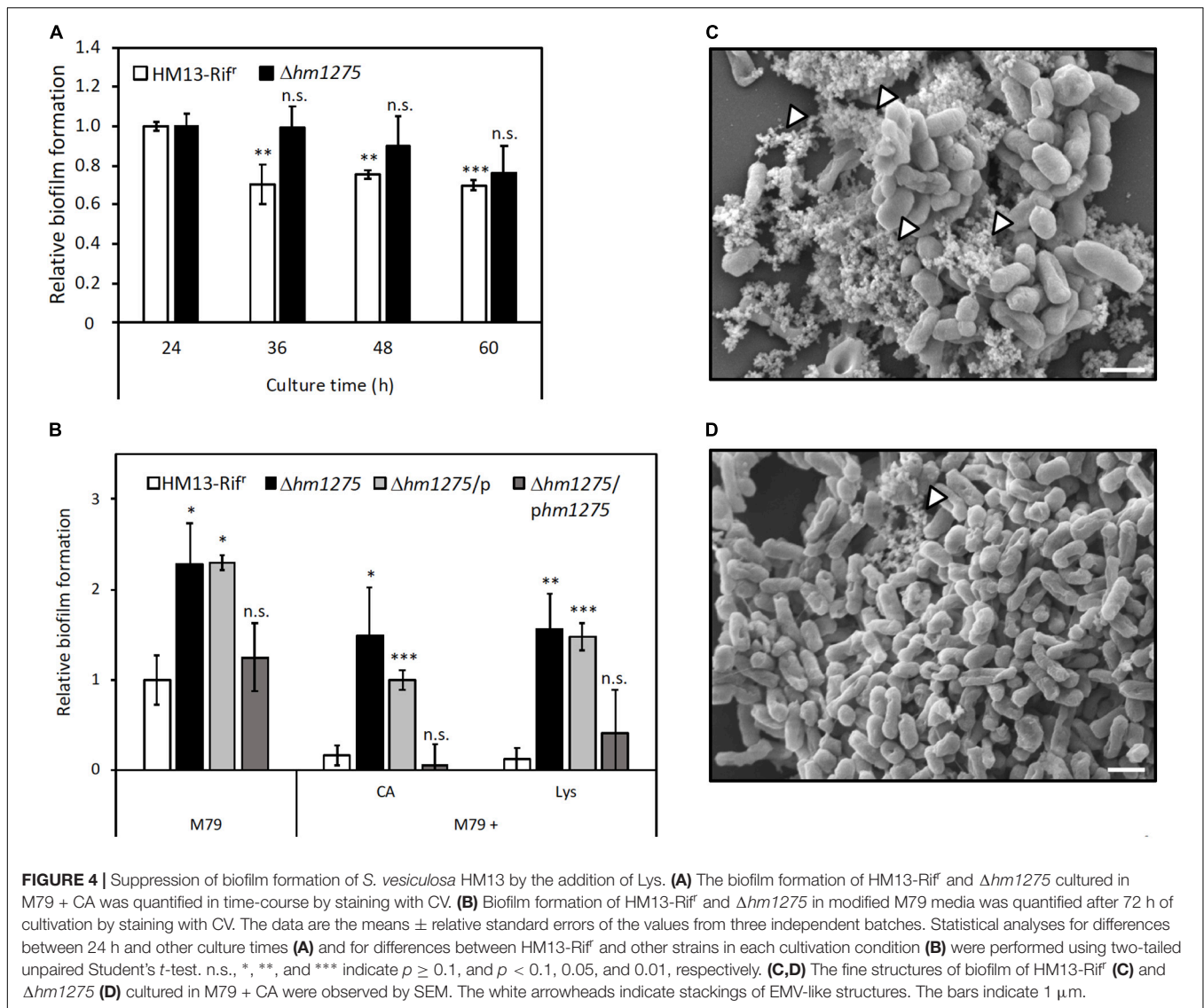
acid sequences with Clustal Omega⁶ (Sievers et al., 2011) revealed that HM1275 has a 38.8% sequence identity to BdlA,

⁶<https://www.ebi.ac.uk/Tools/msa/clustalo/>

a protein related to biofilm dispersion in *P. aeruginosa* PAO1 (accession number: Q9I3S1; **Supplementary Figure 7**; Morgan et al., 2006; Barraud et al., 2009; Petrova and Sauer, 2012). This protein plays a role in sensing the extracellular environment and downregulates the accumulation of cyclic-di-GMP to induce biofilm dispersion. This sequence similarity suggests that HM1275 is not only involved in vesicle production, but also in biofilm formation (Bobrov et al., 2005; Thormann et al., 2006). Therefore, biofilm formation by HM13-Rif^r and $\Delta hm1275$ was measured over time by staining with CV (Thormann et al., 2004). We observed that the amount of biofilm in HM13-Rif^r decreased in a time-dependent manner, but such a decrease was much less significant in the mutant (**Figure 4A**).

To examine whether biofilm formation is controlled by Lys concentration in an HM1275-dependent manner, similar to vesicle production, biofilm formation of HM13-Rif^r and $\Delta hm1275$ cultured in M79 media supplemented with CA and Lys was quantified (**Figure 4B**). Under all conditions tested, the relative amounts of biofilm from HM13-Rif^r were lower than those of $\Delta hm1275$ ($p = 0.067, 0.073,$ and 0.025 for bacteria grown in M79, M79 + CA, and M79 + Lys, respectively) and the empty vector-introduced strain ($\Delta hm1275/p$) ($p = 0.010, 0.0062,$ and 0.0024 for bacteria grown in M79, M79 + CA, and M79 + Lys, respectively), but were not significantly different from those of the complemented strain ($\Delta hm1275/phm1275$). Moreover, the amounts of biofilm from HM13-Rif^r decreased to 16.8% upon addition of CA and to 12.0% upon addition of Lys, whereas those of the mutant decreased by a lesser extent upon addition of CA (65.1%) and Lys (68.3%), compared with those in the original





M79 medium. These results suggest that HM1275 is involved in Lys-induced suppression of biofilm formation.

Next, we analyzed the fine structures of biofilms of HM13-Rif^f and $\Delta hm1275$ by SEM. Some stackings of EMV-like structures were frequently observed in HM13-Rif^f biofilm (white arrowheads in **Figure 4C**). Conversely, such structures were much less frequently observed in the mutant biofilm (white arrowheads in **Figure 4D**).

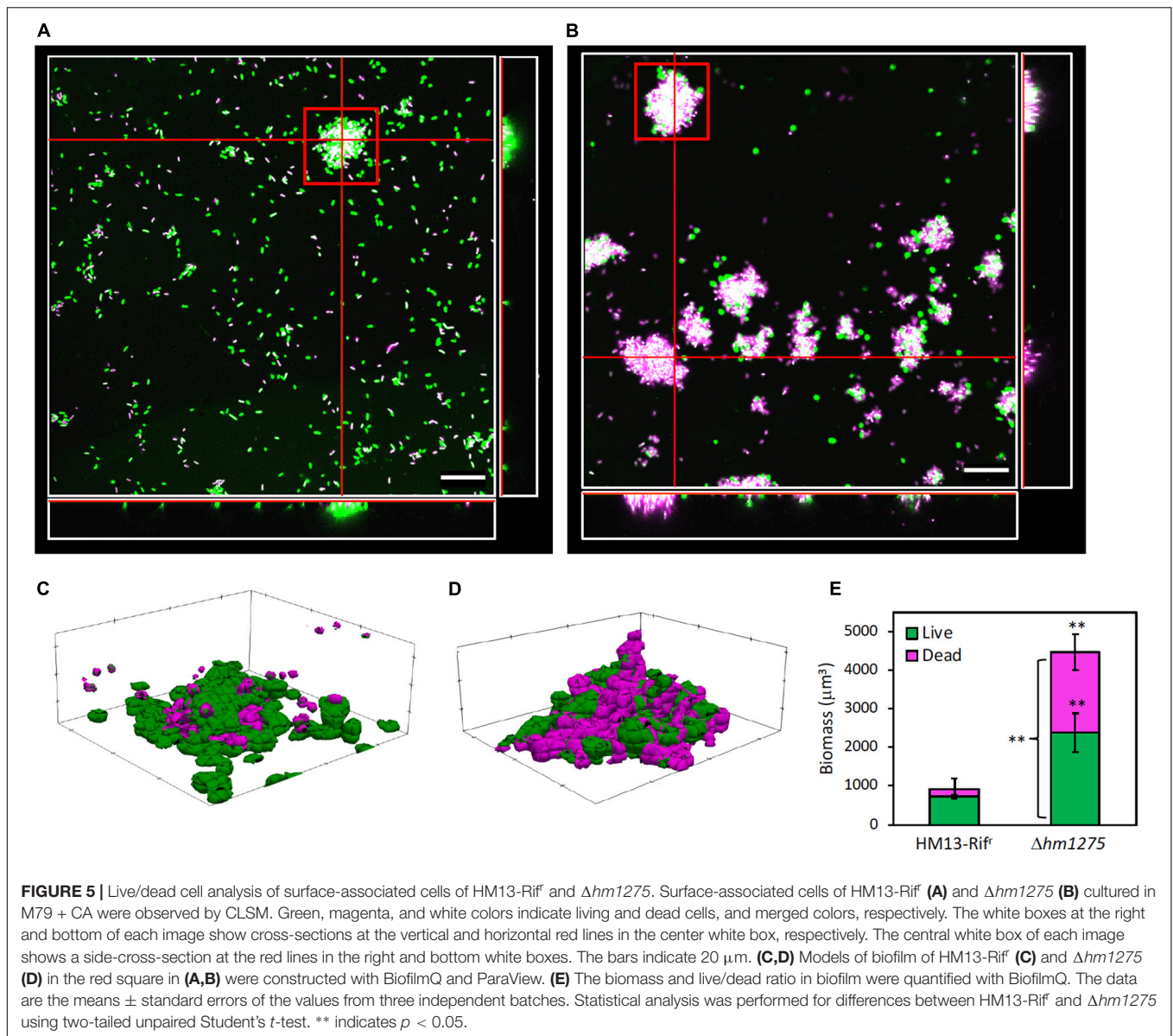
Increased Population of Dead Cells in the Biofilm of $\Delta hm1275$

We further investigated the biomass and live/dead cell ratio in biofilms of HM13-Rif^f and $\Delta hm1275$ by CLSM. For HM13-Rif^f, a small amount of biofilm (red square in **Figure 5A**) and many single cells attached to the glass bottom of the dish base were observed (**Figure 5A**) compared with the mutant, for which a large amount of biofilm was observed (**Figure 5B**). Furthermore, mutant biofilms contained a larger number of dead

cells than HM13-Rif^f biofilms (**Figures 5A,B**). In particular, the sectioned images in CLSM and models of biofilm indicated that the HM13-Rif^f biofilm included a small number of dead cells in its interior region (**Figures 5A,C**), whereas the $\Delta hm1275$ biofilm included abundant dead cells at the bottom and in its interior region (**Figures 5B,D**). Biomass quantification of the biofilm of these strains showed that the total biomass of the mutant biofilm was approximately five-fold larger than that of the HM13-Rif^f biofilm (**Figure 5E**). However, the HM13-Rif^f biofilm was composed of approximately 80% live and 20% dead cells, while the mutant biofilm was composed of approximately 53% live and 47% dead cells.

Comprehensive Identification of Lys-Induced and -Repressed Proteins

To obtain insights into the mechanisms of Lys-induced vesicle production and suppression of biofilm formation mediated by HM1275, proteins up- and downregulated by increasing



the concentration of Lys in the medium from 0.26 to 2.6 g/L were identified by shotgun proteomics (Supplementary Figure 8). Proteome analysis covered approximately 35% of all gene products of *S. vesiculosa* HM13. The genes encoding proteins that showed significant differences in expression levels between cells grown with 0.26 and 2.6 g/L Lys were annotated by a BLAST search and are listed in Table 4. These proteins ($n = 13$) accounted for approximately 1% of the total proteome ($n = 1,488$). Among these proteins, two proteins, a ribosome subunit and a cytochrome *c* oxidase subunit (HM3452 and HM2439, respectively), were slightly upregulated (Table 4). On the other hand, 11 downregulated proteins included proteins related to cell division (HM1357), redox reaction (HM498 and HM4032), transcriptional regulation (HM4030), transportation (HM4042), cell adhesion (HM244), and DNA replication (HM2742)

(Table 4). The possible involvement of these proteins in vesicle production and biofilm formation will be discussed in the “Discussion” section.

DISCUSSION

In this study, we found that the putative sensor protein HM1275 of *S. vesiculosa* HM13 is involved in the regulation of vesicle production and biofilm formation. Vesicle production and suppression of biofilm formation were co-induced through HM1275 in response to high Lys concentrations, suggesting a common regulation mechanism shared between these physiological responses.

To explore the mechanism of HM1275-mediated response to extracellular Lys concentration, we identified proteins whose

expression levels were significantly changed in response to Lys concentration. When the cells were grown with high concentrations of Lys, HM1357, a homolog of a cell division-related protein, BolA, was downregulated (0.56-fold) compared with its expression in cells grown with low concentrations of Lys (Table 4). BolA regulates the transcript levels of several proteins involved in peptidoglycan synthesis, and its deletion causes loss of integrity of the outer membrane (Freire et al., 2006). Furthermore, the deletion of a gene coding for a BolA-like protein, IbaG, reduces peptidoglycan levels and alters outer membrane lipids, disturbing membrane integrity (Fleurie et al., 2019). Decreased membrane peptidoglycan cross-linking plays a role in vesicle formation in Gram-negative bacteria (Nagakubo et al., 2020). Therefore, it is plausible that the downregulated expression of HM1357, a BolA-like protein of *S. vesiculosa* HM13, reduces the stability of the peptidoglycan network and weakens the linkage between peptidoglycan layers and the outer membrane, thereby inducing membrane blebbing and subsequent vesicle production.

We found that HM1275 is also involved in Lys-induced suppression of biofilm formation. Therefore, cells are also supposed to regulate the expression of proteins related to biofilm formation in response to Lys. BolA is also involved in biofilm formation by facilitating the production of fimbria-like adhesins and curli, and negatively modulating flagellar biosynthesis and swimming capacity (Dressaire et al., 2015). Even in the presence of an abundant biofilm-forming factor, cyclic-di-GMP, the absence of BolA reduced the amount of biofilm (Moreira et al., 2017). Therefore, we speculate that HM1275 senses extracellular signals and downregulates the expression of the BolA-like protein HM1357 to suppress biofilm formation.

We also found that HM244, a homolog of a secreted and surface protein containing fasciclin-like repeats, was 0.46-fold downregulated under high Lys conditions (Table 4). The fasciclin domain is involved in cell attachment across plants, animals, and bacteria (Seifert, 2018). Therefore, the decreased production of HM244 in response to high Lys concentration may decrease biofilm formation by suppressing cell adhesion.

Biofilm formation may play an important role in the survival of *S. vesiculosa* HM13 in its original habitat. This strain was isolated from fish intestines, where nutrients fluctuate depending on the feeding activity of the fish; thus, this bacterium should cope well with nutrient fluctuations for its survival (Pereira and Berry, 2017). When nutrients are scarce in the host intestine, biofilm formation is thought to be beneficial for bacterial survival, as reported for various strains (Falkinham, 2009; Cherifi et al., 2017). On the other hand, when the host fish ingests food, the digested food is introduced to the intestine, rendering the environment suitable for bacteria to proliferate. Under these conditions, it is likely that *S. vesiculosa* HM13 cells respond to Lys, which is supposed to be abundant in the diet of the host fish, through the sensor protein HM1275, thereby suppressing biofilm formation. Inside and at the bottom of the biofilm, cells are subjected to low oxygen and nutrient availability (Flemming et al., 2016). Consequently, if the cells cannot properly suppress

biofilm formation under nutrient-rich conditions, they cannot benefit from such conditions and are expected to die because of the limited resources available in the biofilm (Figure 5; Cherifi et al., 2017). Therefore, regulation of biofilm formation in a timely manner, probably by HM1275, contributes to the survival of this strain in a changeable environment.

HM1275 was identified as a cargo of EMVs (Figure 2), although it was predicted to localize to the inner membrane by PSORTb (Yu et al., 2010; Table 3). These results suggest that HM1275 found in the EMV fraction is included in O-IMVs, which display membranes derived from the cell's inner membrane and are produced by various Gram-negative bacteria as a minor fraction of EMVs (Pérez-Cruz et al., 2013, 2015, 2016). This interpretation is supported by our previous observation that *S. vesiculosa* HM13 produces EMVs with a double membrane-bounded structure, which are supposed to be O-IMVs (Chen et al., 2020). On the other hand, the physiological significance of the occurrence of HM1275 in EMVs is currently unknown. As a putative sensor protein, HM1275 is thought to play a role in the cellular inner membrane, where it performs signaling functions that facilitate EMV production and suppression of biofilm formation. Thus, HM1275 packaged into EMVs may not have an active role, but rather be eliminated from the cells as a result of protein quality control (McBroom and Kuehn, 2006) or released into the culture supernatant as a result of explosive cell lysis (Turnbull et al., 2016). Nevertheless, another hypothesis may also be that EMVs function as a carrier of HM1275 for the transfer of this protein to other cells to facilitate collective cell behavior such as the regulation of biofilm formation, although, to our knowledge, the intercellular transfer of inner membrane proteins has not been demonstrated so far. These hypotheses should be examined in future studies. Although the physiological significance of HM1275 in EMVs remains elusive, the present study revealed that a putative sensor protein is involved in nutrient-responsive co-regulation of EMV production and biofilm formation. A possible functional link between EMV production and biofilm formation will also be examined in future studies.

DATA AVAILABILITY STATEMENT

The datasets presented in this study can be found in online repositories. The names of the repository/repositories and accession number(s) can be found below: <https://www.ddbj.nig.ac.jp/>, LC533412 <https://www.ddbj.nig.ac.jp/>, LC533413 <https://www.ddbj.nig.ac.jp/>, LC533414 <https://www.ddbj.nig.ac.jp/>, LC533415 <https://www.ddbj.nig.ac.jp/>, LC533416 <https://www.ddbj.nig.ac.jp/>, LC533417 <https://www.ddbj.nig.ac.jp/>, LC533418 <https://www.ddbj.nig.ac.jp/>, LC533419 <https://www.ddbj.nig.ac.jp/>, LC533420 <https://www.ddbj.nig.ac.jp/>, LC533421 <https://www.ddbj.nig.ac.jp/>, LC533422 <https://www.ddbj.nig.ac.jp/>, LC533423 <https://www.ddbj.nig.ac.jp/>, LC533424 <https://www.ddbj.nig.ac.jp/>, LC533425 <https://www.ddbj.nig.ac.jp/>, LC533426 <https://www.ddbj.nig.ac.jp/>, LC533463 <https://www.ddbj.nig.ac.jp/>, LC547421 <https://www.ddbj.nig.ac.jp/>, LC547422

<https://www.ddbj.nig.ac.jp/>, LC547423 <https://www.ddbj.nig.ac.jp/>, LC547424 <https://www.ddbj.nig.ac.jp/>, LC547425 <https://www.ddbj.nig.ac.jp/>, LC547426 <https://www.ddbj.nig.ac.jp/>, LC533496 <https://www.ddbj.nig.ac.jp/>, LC533506 <https://www.ddbj.nig.ac.jp/>, LC533509 <https://www.ddbj.nig.ac.jp/>, LC533516 <https://www.ddbj.nig.ac.jp/>, LC533517 <https://www.ddbj.nig.ac.jp/>, LC533518.

AUTHOR CONTRIBUTIONS

FY, JK, and TK designed the study, discussed the results, and wrote the manuscript. FY performed the experiments. TI contributed to electron microscopic analysis. WA and MU contributed to proteome analysis. All authors have read and approved the submitted version.

FUNDING

This work was supported by research grants from the JSPS KAKENHI (JP15H04474, JP17H04598, JP18H02127, JP18K19178, and JP20K20570 to TK and JP16K14885 to JK),

REFERENCES

- Alexeyev, M. F. (1999). The pKNOCK series of broad-host-range mobilizable suicide vectors for gene knockout and targeted DNA insertion into the chromosome of Gram-negative bacteria. *BioTechniques* 26, 824–828. doi: 10.2144/99265bm05
- Altschul, S. F., Madden, T. L., Schäffer, A. A., Zhang, J., Zhang, Z., Miller, W., et al. (1997). Gapped BLAST and PSI-BLAST: a new generation of protein database search programs. *Nucleic Acids Res.* 25, 3389–3402. doi: 10.1093/nar/25.17.3389
- Barraud, N., Schleheck, D., Klebensberger, J., Webb, J. S., Hassett, D. J., Rice, S. A., et al. (2009). Nitric oxide signaling in *Pseudomonas aeruginosa* biofilms mediates phosphodiesterase activity, decreased cyclic di-GMP levels, and enhanced dispersal. *J. Bacteriol.* 191, 7333–7342. doi: 10.1128/jb.00975-09
- Bitto, N., and Kaparakis-Liaskos, M. (2017). The therapeutic benefit of bacterial membrane vesicles. *Int. J. Mol. Sci.* 18:1287. doi: 10.3390/ijms18061287
- Bobrov, A. G., Kirillina, O., and Perry, R. D. (2005). The phosphodiesterase activity of the HmsP EAL domain is required for negative regulation of biofilm formation in *Yersinia pestis*. *FEMS Microbiol. Lett.* 247, 123–130. doi: 10.1016/j.femsle.2005.04.036
- Chen, C., Kawamoto, J., Kawai, S., Tame, A., Kato, C., Imai, T., et al. (2020). Isolation of a novel bacterial strain capable of producing abundant extracellular membrane vesicles carrying a single major cargo protein and analysis of its transport mechanism. *Front. Microbiol.* 10:3001. doi: 10.3389/fmicb.2019.03001
- Chen, Y.-C., Tou, J. C., and Jaczynski, J. (2009). Amino acid and mineral composition of protein and other components and their recovery yields from whole antarctic krill (*Euphausia superba*) using isoelectric solubilization/precipitation. *J. Food Sci.* 74, H31–H39. doi: 10.1111/j.1750-3841.2008.01026.x
- Cherifi, T., Jacques, M., Quessy, S., and Fravallo, P. (2017). Impact of nutrient restriction on the structure of *Listeria monocytogenes* biofilm grown in a microfluidic system. *Front. Microbiol.* 8:864. doi: 10.3389/fmicb.2017.00864
- Choi, Y., Kim, S., Hwang, H., Kim, K.-P., Kang, D.-H., and Ryu, S. (2015). Plasmid-encoded MCP is involved in virulence, motility, and biofilm formation of *Cronobacter sakazakii* ATCC 29544. *Infect. Immun.* 83, 197–204. doi: 10.1128/iai.02633-14

the Institute for Fermentation, Osaka (L-2019-2-012 to TK), and JSPS Research Fellowship for Young Scientists (to FY).

ACKNOWLEDGMENTS

We thank Prof. Hiroyuki Yano (Research Institute for Sustainable Humanosphere, Kyoto University) for SEM observation of bacterial biofilm; Prof. Shiroh Futaki and Dr. Kenichi Kawano (Institute for Chemical Research, Kyoto University) for CLSM analysis of bacterial biofilm; Prof. Kazunari Akiyoshi and Dr. Asako Shimoda (Graduate School of Engineering, Kyoto University) for nanoparticle tracking analysis of bacterial vesicles. Transmission electron microscopy was performed in collaboration with the Analysis and Development System for Advanced Materials (ADAM) at the Research Institute for Sustainable Humanosphere, Kyoto University.

SUPPLEMENTARY MATERIAL

The Supplementary Material for this article can be found online at: <https://www.frontiersin.org/articles/10.3389/fmicb.2021.629023/full#supplementary-material>

- Dressaire, C., Moreira, R. N., Barahona, S., Matos, A. P. A., and Arraiano, C. M. (2015). BolA is a transcriptional switch that turns off motility and turns on biofilm development. *mBio* 6, 2352–2314e. doi: 10.1128/mbio.02352-14
- Falke, J. J., Bass, R. B., Butler, S. L., Chervitz, S. A., and Danielson, M. A. (1997). The two-component signaling pathway of bacterial chemotaxis: a molecular view of signal transduction by receptors, kinases, and adaptation enzymes. *Annu. Rev. Cell Dev. Biol.* 13, 457–512. doi: 10.1146/annurev.cellbio.13.1.457
- Falkinham, J. O. III (2009). Surrounded by mycobacteria: nontuberculous mycobacteria in the human environment. *J. Appl. Microbiol.* 107, 356–367. doi: 10.1111/j.1365-2672.2009.04161.x
- Filipe, V., Hawe, A., and Jiskoot, W. (2010). Critical evaluation of nanoparticle tracking analysis (NTA) by NanoSight for the measurement of nanoparticles and protein aggregates. *Pharmaceut. Res.* 27, 796–810. doi: 10.1007/s11095-010-0073-2
- Flemming, H.-C., Wingender, J., Szewzyk, U., Steinberg, P., Rice, S. A., and Kjelleberg, S. (2016). Biofilms: an emergent form of bacterial life. *Nat. Rev. Microbiol.* 14:563. doi: 10.1038/nrmicro.2016.94
- Fleurie, A., Zoued, A., Alvarez, L., Hines, K. M., Cava, F., Xu, L., et al. (2019). A *Vibrio cholerae* BolA-like protein is required for proper cell shape and cell envelope integrity. *mBio* 10, 790–719e. doi: 10.1128/mbio.00790-19
- Freire, P., Vieira, H. L. A., Furtado, A. R., Pedro, M. A., and Arraiano, C. M. (2006). Effect of the morphogene *bolA* on the permeability of the *Escherichia coli* outer membrane. *FEMS Microbiol. Lett.* 260, 106–111. doi: 10.1111/j.1574-6968.2006.00307.x
- Guida, R. D., Casillo, A., Yokoyama, F., Kawamoto, J., Kurihara, T., and Corsaro, M. M. (2020). Detailed structural characterization of the lipooligosaccharide from the extracellular membrane vesicles of *Shewanella vesiculosa* HM13. *Mar. Drugs* 18:231. doi: 10.3390/md18050231
- Hanlon, D. W., and Ordal, G. W. (1994). Cloning and characterization of genes encoding methyl-accepting chemotaxis proteins in *Bacillus subtilis*. *J. Biol. Chem.* 269, 14038–14046.
- Hartmann, R., Jeckel, H., Jelli, E., Singh, P. K., Vaidya, S., Bayer, M., et al. (2019). BiofilmQ, a software tool for quantitative image analysis of microbial biofilm communities. *bioRxiv* 2019:735423. doi: 10.1101/735423
- Hedblom, M. L., and Adler, J. (1980). Genetic and biochemical properties of *Escherichia coli* mutants with defects in serine chemotaxis. *J. Bacteriol.* 144, 1048–1060.

- Henry, J. T., and Crosson, S. (2011). Ligand-binding PAS domains in a genomic, cellular, and structural context. *Annu. Rev. Microbiol.* 65, 261–286. doi: 10.1146/annurev-micro-121809-151631
- Huntley, M. E., Nordhausen, W., and Lopez, M. D. G. (1994). Elemental composition, metabolic activity and growth of Antarctic krill *Euphausia superba* during winter. *Mar. Ecol. Prog. Ser.* 107, 23–40. doi: 10.3354/meps107023
- Iwamoto, S., Nakagaito, A. N., and Yano, H. (2007). Nano-fibrillation of pulp fibers for the processing of transparent nanocomposites. *Appl. Phys.* 89, 461–466. doi: 10.1007/s00339-007-4175-6
- Jain, S., and Pillai, J. (2017). Bacterial membrane vesicles as novel nanosystems for drug delivery. *Int. J. Nanomed.* 12, 6329–6341. doi: 10.2147/IJN.S137368
- Jardas, I., Šantić, M., and Pallaoro, A. (2004). Diet composition and feeding intensity of horse mackerel, *Trachurus trachurus* (Osteichthyes: Carangidae) in the eastern Adriatic. *Mar. Biol.* 144, 1051–1056. doi: 10.1007/s00227-003-1281-7
- Kamasaka, K., Kawamoto, J., Chen, C., Yokoyama, F., Imai, T., Ogawa, T., et al. (2020). Genetic characterization and functional implications of the gene cluster for selective protein transport to extracellular membrane vesicles of *Shewanella vesiculosa* HM13. *Biochem. Biophys. Res. Commun.* 526, 525–531. doi: 10.1016/j.bbrc.2020.03.125
- Kawano, K., Yokoyama, F., Kawamoto, J., Ogawa, T., Kurihara, T., and Futaki, S. (2020). Development of a simple and rapid method for *in situ* vesicle detection in cultured media. *J. Mol. Biol.* 432, 5876–5888. doi: 10.1016/j.jmb.2020.09.009
- Kolmakova, A., and Kolmakov, V. (2019). Amino acid composition of green microalgae and diatoms, cyanobacteria, and zooplankton. *Inland Water Biol.* 12, 452–461. doi: 10.1134/s1995082919040060
- Manning, A. J., and Kuehn, M. J. (2011). Contribution of bacterial outer membrane vesicles to innate bacterial defense. *BMC Microbiol.* 11:258. doi: 10.1186/1471-2180-11-258
- McBroom, A. J., and Kuehn, M. J. (2006). Release of outer membrane vesicles by Gram-negative bacteria is a novel envelope stress response: outer membrane vesicles relieve envelope stress. *Mol. Microbiol.* 63, 545–558. doi: 10.1111/j.1365-2958.2006.05522.x
- Moreira, R. N., Dressaire, C., Barahona, S., Galego, L., Kaeffer, V., Jenal, U., et al. (2017). BolA is required for the accurate regulation of c-di-GMP, a central player in biofilm formation. *mBio* 8, 443–417e. doi: 10.1128/mbio.00443-17
- Morgan, R., Kohn, S., Hwang, S.-H., Hassett, D. J., and Sauer, K. (2006). BdlA, a chemotaxis regulator essential for biofilm dispersion in *Pseudomonas aeruginosa*. *J. Bacteriol.* 188, 7335–7343. doi: 10.1128/jb.00599-06
- Nagakubo, T., Nomura, N., and Toyofuku, M. (2020). Cracking open bacterial membrane vesicles. *Front. Microbiol.* 10:3026. doi: 10.3389/fmicb.2019.03026
- Orench-Rivera, N., and Kuehn, M. J. (2016). Environmentally controlled bacterial vesicle-mediated export. *Cell Microbiol.* 18, 1525–1536. doi: 10.1111/cmi.12676
- Papa, R., Glagla, S., Danchin, A., Schweder, T., Marino, G., and Duilio, A. (2006). Proteomic identification of a two-component regulatory system in *Pseudoalteromonas haloplanktis* TAC125. *Extremophiles* 10, 483–491. doi: 10.1007/s00792-006-0525-0
- Park, J., Kawamoto, J., Esaki, N., and Kurihara, T. (2012). Identification of cold-inducible inner membrane proteins of the psychrotrophic bacterium, *Shewanella livingstonensis* Ac10, by proteomic analysis. *Extremophiles* 16:227. doi: 10.1007/s00792-011-0422-z
- Pereira, F. C., and Berry, D. (2017). Microbial nutrient niches in the gut. *Environ. Microbiol.* 19, 1366–1378. doi: 10.1111/1462-2920.13659
- Pérez-Cruz, C., Cañas, M.-A., Giménez, R., Badia, J., Mercade, E., Baldomà, L., et al. (2016). Membrane vesicles released by a hypervesiculating *Escherichia coli* Nissle 1917 *tolR* mutant are highly heterogeneous and show reduced capacity for epithelial cell interaction and entry. *PLoS One* 11:e0169186. doi: 10.1371/journal.pone.0169186
- Pérez-Cruz, C., Carrión, O., Delgado, L., Martínez, G., López-Iglesias, C., Mercade, E., et al. (2013). New type of outer membrane vesicle produced by the Gram-negative bacterium *Shewanella vesiculosa* M7^T: implications for DNA content. *Appl. Environ. Microbiol.* 79:1874. doi: 10.1128/AEM.03657-12
- Pérez-Cruz, C., Delgado, L., López-Iglesias, C., and Mercade, E. (2015). Outer-inner membrane vesicles naturally secreted by Gram-negative pathogenic bacteria. *PLoS One* 10:e0116896. doi: 10.1371/journal.pone.0116896
- Petrova, O. E., and Sauer, K. (2012). PAS domain residues and prosthetic group involved in BdlA-dependent dispersion response by *Pseudomonas aeruginosa* biofilms. *J. Bacteriol.* 194, 5817–5828. doi: 10.1128/jb.00780-12
- Rath, A., and Deber, C. M. (2013). Correction factors for membrane protein molecular weight readouts on sodium dodecyl sulfate-polyacrylamide gel electrophoresis. *Anal. Biochem.* 434, 67–72. doi: 10.1016/j.ab.2012.11.007
- Rath, A., Glibowicka, M., Nadeau, V. G., Chen, G., and Deber, C. M. (2009). Detergent binding explains anomalous SDS-PAGE migration of membrane proteins. *Proc. Natl. Acad. Sci. U S A.* 106, 1760–1765. doi: 10.1073/pnas.0813167106
- Rossi, E., Paroni, M., and Landini, P. (2018). Biofilm and motility in response to environmental and host-related signals in Gram negative opportunistic pathogens. *J. Appl. Microbiol.* 125, 1587–1602. doi: 10.1111/jam.14089
- Sabaiefard, P., Abdi-Ali, A., Gamazo, C., Irache, J. M., and Soudi, M. R. (2017). Improved effect of amikacin-loaded poly(D,L-lactide-co-glycolide) nanoparticles against planktonic and biofilm cells of *Pseudomonas aeruginosa*. *J. Med. Microbiol.* 66, 137–148. doi: 10.1099/jmm.0.000430
- Schwechheimer, C., and Kuehn, M. J. (2015). Outer-membrane vesicles from Gram-negative bacteria: biogenesis and functions. *Nat. Rev. Microbiol.* 13, 605–619. doi: 10.1038/nrmicro3525
- Seifert, G. J. (2018). Fascinating fasciclins: a surprisingly widespread family of proteins that mediate interactions between the cell exterior and the cell surface. *Int. J. Mol. Sci.* 19:1628. doi: 10.3390/ijms19061628
- Sievers, F., Wilm, A., Dineen, D., Gibson, T. J., Karplus, K., Li, W., et al. (2011). Fast, scalable generation of high-quality protein multiple sequence alignments using Clustal Omega. *Mol. Syst. Biol.* 7:539. doi: 10.1038/msb.2011.75
- Simon, R., Priefer, U., and Pühler, A. (1983). A broad host range mobilization system for *in vivo* genetic engineering: transposon mutagenesis in Gram negative bacteria. *Bio/Technology* 1, 784–791. doi: 10.1038/nbt1183-784
- Söding, J., Biegert, A., and Lupas, A. N. (2005). The HHpred interactive server for protein homology detection and structure prediction. *Nucleic Acids Res.* 33, 244–248. doi: 10.1093/nar/gki408
- Springer, M. S., Goy, M. F., and Adler, J. (1977). Sensory transduction in *Escherichia coli*: two complementary pathways of information processing that involve methylated proteins. *Proc. Natl. Acad. Sci. U S A.* 74, 3312–3316. doi: 10.1073/pnas.74.8.3312
- Tan, K., Li, R., Huang, X., and Liu, Q. (2018). Outer membrane vesicles: current status and future direction of these novel vaccine adjuvants. *Front. Microbiol.* 9:783. doi: 10.3389/fmicb.2018.00783
- Thormann, K. M., Duttler, S., Saville, R. M., Hyodo, M., Shukla, S., Hayakawa, Y., et al. (2006). Control of formation and cellular detachment from *Shewanella oneidensis* MR-1 biofilms by cyclic di-GMP. *J. Bacteriol.* 188, 2681–2691. doi: 10.1128/jb.188.7.2681-2691.2006
- Thormann, K. M., Saville, R. M., Shukla, S., Pelletier, D. A., and Spormann, A. M. (2004). Initial phases of biofilm formation in *Shewanella oneidensis* MR-1. *J. Bacteriol.* 186, 8096–8104. doi: 10.1128/jb.186.23.8096-8104.2004
- Toyofuku, M., Tashiro, Y., Hasegawa, Y., Kurosawa, M., and Nomura, N. (2015). Bacterial membrane vesicles, an overlooked environmental colloid: biology, environmental perspectives and applications. *Adv. Colloid Interface Sci.* 226, 65–77. doi: 10.1016/j.cis.2015.08.013
- Toyotake, Y., Cho, H.-N., Kawamoto, J., and Kurihara, T. (2018). A novel 1-acyl-sn-glycerol-3-phosphate O-acyltransferase homolog for the synthesis of membrane phospholipids with a branched-chain fatty acyl group in *Shewanella livingstonensis* Ac10. *Biochem. Biophys. Res. Commun.* 500, 704–709. doi: 10.1016/j.bbrc.2018.04.140
- Tsuji, T., Ozasa, H., Aoki, W., Aburaya, S., Funazo, T. Y., Furugaki, K., et al. (2020). YAP1 mediates survival of ALK-rearranged lung cancer cells treated with alectinib via pro-apoptotic protein regulation. *Nat. Commun.* 11:74. doi: 10.1038/s41467-019-13771-5
- Turnbull, L., Toyofuku, M., Hynen, A. L., Kurosawa, M., Pessi, G., Petty, N. K., et al. (2016). Explosive cell lysis as a mechanism for the biogenesis of bacterial membrane vesicles and biofilms. *Nat. Commun.* 7:11220. doi: 10.1038/ncomms11220
- Ud-Din, A. I. M. S., and Roujeinikova, A. (2017). Methyl-accepting chemotaxis proteins: a core sensing element in prokaryotes and archaea. *Cell Mol. Life Sci.* 74, 3293–3303. doi: 10.1007/s00018-017-2514-0

- Wadhams, G. H., and Armitage, J. P. (2004). Making sense of it all: bacterial chemotaxis. *Nat. Rev. Mol. Cell Bio.* 5, 1024–1037. doi: 10.1038/nrm1524
- Yokoyama, F., Kawamoto, J., Imai, T., and Kurihara, T. (2017). Characterization of extracellular membrane vesicles of an Antarctic bacterium, *Shewanella livingstonensis* Ac10, and their enhanced production by alteration of phospholipid composition. *Extremophiles* 21, 723–731. doi: 10.1007/s00792-017-0937-z
- Yu, N. Y., Wagner, J. R., Laird, M. R., Melli, G., Rey, S., Lo, R., et al. (2010). PSORTb 3.0: improved protein subcellular localization prediction with refined localization subcategories and predictive capabilities for all prokaryotes. *Bioinformatics* 26, 1608–1615. doi: 10.1093/bioinformatics/btq249

Conflict of Interest: The authors declare that the research was conducted in the absence of any commercial or financial relationships that could be construed as a potential conflict of interest.

Copyright © 2021 Yokoyama, Imai, Aoki, Ueda, Kawamoto and Kurihara. This is an open-access article distributed under the terms of the Creative Commons Attribution License (CC BY). The use, distribution or reproduction in other forums is permitted, provided the original author(s) and the copyright owner(s) are credited and that the original publication in this journal is cited, in accordance with accepted academic practice. No use, distribution or reproduction is permitted which does not comply with these terms.